Ocean Wave Forecasting in the Gulf of Thailand during Typhoon Linda 1997 : WAM and Neural Network Approaches

Wattana Kanbua[a]*, Seree Supharatid[b], and I-Ming Tang[c]

[a] Department of Mathematics, Faculty of Science, Mahidol University, Bangkok 10400, Thailand.
[b] Natural Disaster Research Center, College of Engineering, Rangsit University, Pathumhani 12000, Thailand.
[c] Department of Physics, Faculty of Science, Mahidol University, Bangkok 10400, Thailand.

* Corresponding author, E-mail: watt_kan@hotmail.com, watt_kan@yahoo.com

ABSTRACT: This paper presents an investigation of wave field during the attack of typhoon Linda in 1997 in the Gulf of Thailand. Two modeling approaches are studied: The hard computing approach by the WAM cycle 4 model was used firstly to simulate wave heights and periods distribution covering the domain 95°E to 105°E and 5°N to 15°N. Then, the soft computing approach by the GRNN model was developed to predict the wave characteristics for lead times of 3, 6, 9, 12, and 24 hrs. The input wind data were obtained from NOGAPS model archives with 1 degree resolution and are linearly interpolated to specify wind components at each grid points. It was found that the WAM model underestimated the wave height as much as 20%. The root mean square errors (RMSE) and the mean absolute deviations (MAD) are 0.18 – 0.26 m and 0.13 – 0.18 m, respectively. The GRNN showed better forecasting results than the WAM model (RMSE < 0.15 m and MAD <0.10 m). The maximum wave height simulated by the GRNN model during the typhoon Linda 1997 event was found to be 4.0 m while the observed data was 4.06 m. This indicates that for short-term prediction within 24 hrs, the data-driven model such as the GRNN should be viewed as a strong alternative in operational forecasting.

KEYWORDS: WAM cycle 4, General Regression Neural Network (GRNN), typhoon Linda.

INTRODUCTION

The Gulf of Thailand is located in Southeast Asia, immediately to the west of the South China Sea. Its bordering nations, Cambodia, Malaysia, Thailand, and Vietnam, have each historically profited from the Gulf's wealth of living and mineral resources. Millions of people derive their livelihoods from fish and petroleum harvested from the Gulf, and millions more are affected by changes in the environment of the Gulf, whether physical or political.

The pattern of surface wind directions is characterized by the monsoon system. The prevailing winds during the northeast monsoon season are mostly northeasterly, while it is southwesterly over the Gulf of Thailand during the southwest monsoon. Tropical cyclones affecting Thailand usually move from the western North Pacific Ocean or the South China Sea. Their strength may be characterized by wind speed. The Gulf of Thailand normally receives the effect of tropical depressions because of its location farther inland and because some mountain ranges which obstruct and decrease the wind speed before moving towards the Gulf.

This study concerns the short-term prediction of wave characteristics in the Gulf of Thailand. The wave fields were selected to cover the tropical cyclone event from August 1st to December 31st, 1997. At that time typhoon Linda occurred in the Gulf of Thailand during the 1st – 4th of November, 1997 which the wave buoy reported to be 4.06 m of significant wave height. Two approaches are investigated, namely the hard computing technique by the WAM cycle 4.0 model and the soft computing technique by the general regression neural network model (GRNN).

The WAM Cycle 4.0

The WAM model, which was developed by WAMDI-group[1] and improved by Komen et al. (1994)[2], is one of the best-tested wave models. It is widely used for global and regional operational wave forecasting in many marine and meteorological centers around the world, such as global operational wave forecasting at the European Centre for Medium-Range Weather Forecast.

The model runs for any given regional and global grid with a prescribed topographic data set. The grid resolution can be arbitrary in space and time. The computation can be done on a latitudinal-longitudinal or on a cartesian grid. The model outputs are significant wave height, mean wave direction and frequency, wind stress fields including the wave induced stress, the drag coefficient and 2D wave spectrum at any selected grid points and time.

The WAM model is free for non-commercial use. In this paper we use the latest version[3] which includes a new wind input parameterization developed by Janssen (1991)[4].

The WAM model solves the wave action density transport equation without predefined spectral constraints. The model is applicable in a broad range of wave conditions, ranging from quite daily to tropical cyclone wave conditions. As described in Komen et al. (1994)[2] this wave model solves the transport equation of the directional wave spectrum (Eq. (1)).

$$\frac{dF}{dt} + \frac{\partial(\dot{\phi}F)}{\partial\phi} + \frac{\partial(\dot{\lambda}F)}{\partial\lambda} + \frac{\partial(\dot{\theta}F)}{\partial\theta} = S \qquad (1)$$

where F represents the spectral density with respect to (f,θ,ϕ,λ), f denotes frequencies, θ is the wave direction, ϕ and λ are the latitude and longitude, respectively, and $\dot{\phi}$, $\dot{\lambda}$, $\dot{\theta}$ are the rate of change of the position and propagation direction of a wave packet traveling along a great circle path. For the source terms, represents a superposition of the wind input, S_{in}, white capping dissipation, S_{dis}, and nonlinear transfer function, S_{nl} (see Eq. (2)).

$$S = S_{in} + S_{dis} + S_{nl} \qquad (2)$$

The wind input term was adopted from Snyder et al. (1981)[5]. Wind input and dissipation terms of the present cycle 4 of the wave model are a further de-velopment based on Janssen's quasi-linear theory of wind-wave generation[6,7]. The dissipation source term is based on Hasselmann et al. (1974)[7] white capping theory. The nonlinear source term is a parameterization of the exact nonlinear interactions as proposed by Hasselmann et al. (1985)[8]. The basic form of the exact nonlinear expression is retained. However the five-dimensional continuum of all resonant quadruplets is reduced to a two-dimensional continuum by considering only a pair of discrete interaction configurations.

The WAM model can be used, in principle, for deep and shallow water conditions, considering (or not) depth and current refraction. Extensively applied and tested for different meteorological conditions, it has a well established performance envelope. However, one of the limitations of WAM appears when the propagation time step is larger that the source term integration time step (usually for high spatial resolutions in shallow waters). The small time step for propagation, requires a small time step for the source term integration and is consequently excessive and impractical[9]. Another limitation is that typical physical processes of shallow water waves are not considered in WAM cycle 4.0 (Diffraction, triad-wave interactions, depth-induced wave breaking, etc). The high-resolution model for the Gulf of Thailand was nested into a coarse global model with swell from the South China Sea being allowed to propagate into the Gulf of Thailand.

The integration of the source terms was performed with an implicit scheme while the propagation term was done by the first order upwind flux scheme. The CPU time and memory usage depended on the region of interest and the grid resolution. In this study 20 hours of CPU time are needed for a 5 month simulation using a Pentium IV 2.6 GHz (OS on Linux system) on a 0.25 by 0.25 degree lat-long grid, 25 frequencies, and 12 directions.

The GRNN Model

Use of neural network (NN) techniques to solve problems in civil engineering began in the late 1980s.[10] Their applications to simulating and forecasting problems in water resources are few and relatively recent.[11,12,13,14,15,16,17] The NN modeling techniques used to solve oceanographic problems are also a relatively new area of research.[18,19,20,21,22] Unlike other conventional-based models, the NN model is able to solve problems without any prior assumptions. As long as enough data are available, the NN will extract any regularities or patterns that may exist and use it to form a relationship between input and output. Additional benefits include data error tolerance and the characteristic of being data-driven, thereby providing a capacity to learn and generalize patterns in noisy and ambiguous input data.

The GRNN is the NN architecture that can solve any function approximation problems in the sense of estimating a probability distribution function. The network was firstly developed by Specht (1991)[23]. The learning process is equivalent to finding a surface in a multidimensional space that provides a best fit being measured by some statistical parameters. In GRNN, projected outputs are weighted according to the distance in the phase space between the input pattern and the learning pattern.

The GRNN is a three-layer network with one hidden layer as described in Fig. 1. Each layer has entirely different roles:

·The input layer is where the inputs are applied.

·The hidden layer is where a nonlinear transformation is applied on the data from the input space to the hidden space. In most applications the hidden space is of high dimensionality.

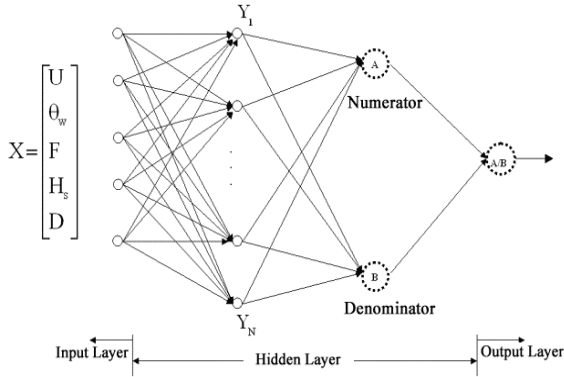·The linear output layer is where the outputs are produced.
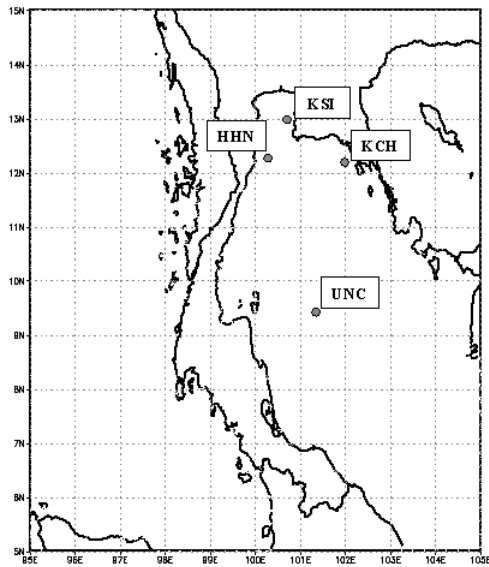

Fig 1. GRNN architecture.

Fig 2. Study area.

The input is a state space denoted by $X_t(U_{10}, \theta_w, F_L, H_s, D_w)$, where U_{10} is wind velocity at 10 m above the mean sea level, θ_w is wind direction, F_L is fetch length, H_s is significant wave height, D_w is sea depth and the desired output is the future value, Y_{t+T}. The future prediction value (O_{t+T}) is calculated by Eq. (3).

$$O_{t+T} = \frac{\sum_{i=1}^{N} Y_{t+T} \, exp(-\frac{D_i^2}{2\sigma^2})}{\sum_{i=1}^{N} exp(-\frac{D_i^2}{2\sigma^2})} \qquad (3)$$
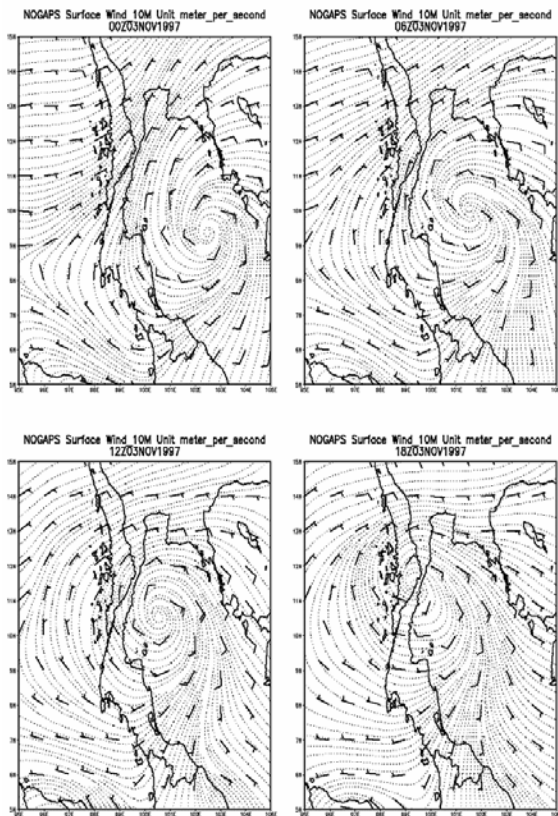
where N is the number of input vectors, D_i^2 is a scalar function representing the Euclidean square distance from the new input vector to the training input vector, and σ is a single smoothing parameter which determines how tightly the network matches its predictions to the data in the training patterns.
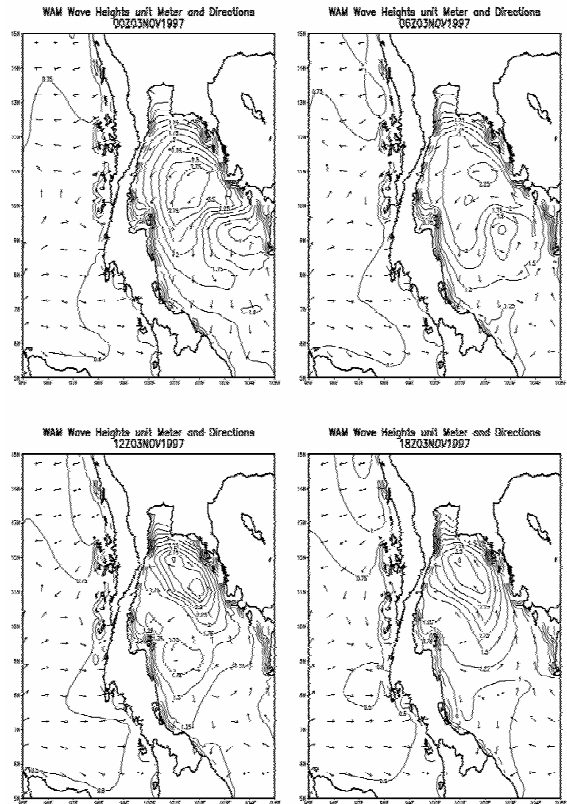
DATA OBSERVATIONS AND SIMULATION RESULTS

Bathymetry grid is taken from ETOPO5[24] covering the region 95°E to 105°E and 5°N to 15°N (see Fig. 2) with 0.25 degree resolution in both latitude and longitude (41 x 41 grids). The initially employed wind data (from the Navy Operational Global Atmospheric Prediction System (NOGAPS) Model[25] archives) were provided by the Naval Research Laboratory Monterey (NRLMRY). The winds are from the period 00Z 1-8-97 to 00Z 31-12-97, with 1.0° resolution and are linearly interpolated to specify wind components at each wave grid point. During the 1st – 4th of November 1997, strong northeasterly winds associated with a significant tropical cyclone activity were observed in the Gulf of Thailand. The wind speed reached up to 22 m/s over the area of study. Wave data were obtained from 3 moored buoys of GISTDA (HHN, KCH, and KSI stations) and 1 automatic marine meteorological station (UNC station). Time and space scales of model and measurements were made comparable by taking appropriate averages.

The wave hindcasting was carried out using 12 directional bands, 25 frequency bands and frequency interval extending from 0.042 to 0.41 Hz. A 5-minute time step has been used for the integration of advection and source terms, considering depth refraction. The output time step was 6 hours and a JONSWAP spectrum was selected as an initial condition. The wind data during November 1st – 4th, 1997 was used to investigate the generated wave fields under the typhoon event. Wind fields, significant wave heights and peak wave periods are shown every 6 hours in Figs. 3 to 6, respectively. The wind and wave directions are plotted using the meteorological convention with arrows every 10 grid points.

Figure 3 shows the wind input (NOGAPS), characterized by the speed and direction. On November 3rd, 1997, the wind field at 00 UTC was uniform along the shoreline with speeds approximately 10 m/s. The simultaneous wave fields displayed 2.0 m height with the maximum of 3.6 m near the storm center. Six hours later (at 06 UTC), the wind fields became more well organized with a speed of 12 m/s and 18 m/s along the shoreline and near the storm center, respectively. The storm still kept moving to the west and hit land at 18, UTC. Wave heights of about 4.5 m were observed near the shoreline. Generally, the wave fields follow the wind

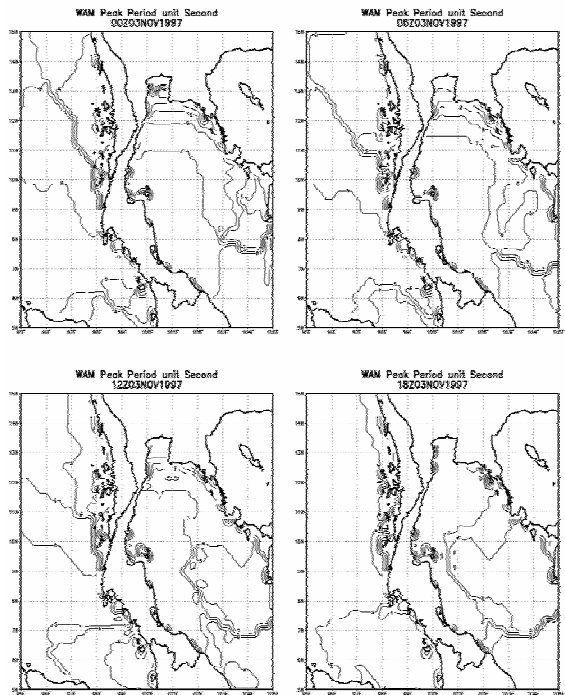**Fig 3.** Wind fields on November 3rd, 1997 every 6 hours (NOGAPS).

Fig 4. Wave fields on November 3rd, 1997 every 6 hours (WAM output).

patterns rather well. Comparing the wind fields in Fig. 3 and wave fields in Fig. 4, the spatial variability is closely related. The maximums of H_s are associated with the maximum wind speeds.

A sequence of peak wave period is shown in Fig. 5. On November 3rd, 1997, during the first 6 hours, the region of simulation was characterized by mainly sea waves. Under the strong north-easterly winds, a 9-second swell was generated and distributed along the south coast. It reached the UNC station at 00 UTC. This swell was further advected to the north, arriving at the HHN station with 10-second peak wave periods at 12 UTC. Six hours later it arrived in the upper region of the Gulf.

Comparison of wave height and wave period time series at the HHN station is shown in Fig. 6. In general, the modeled wave heights underestimate the observed wave heights especially in extreme cases where underestimation reaches 20 %. The wave buoy reported the maximum of 4.06 m significant wave height, whereas the simulated value is approximately 3.2 m at 06 UTC on November 3rd, 1997. Difference of nearly 1 m wave height can be attributed to: i) the limited "local" quality of the wind field (since the NOGAPS wind data correspond to a grid size of 1.0° resolution while the

Fig 5. Peak period maps on November 3rd, 1997 (WAM output).

WAM model grid size is 0.25°) and ii) the enhanced energy dissipation due to the centered differences used in the model and the relatively close presence of a "diagonal" boundary. The comparison in term of the time series peak wave period also reveals that during the first 481 hours there were mainly sea waves. After this time the peak period increased to 6 s (Buoy data) and 7.4 s (WAM), denoting a clear effect of typhoon Linda winds on swell waves.
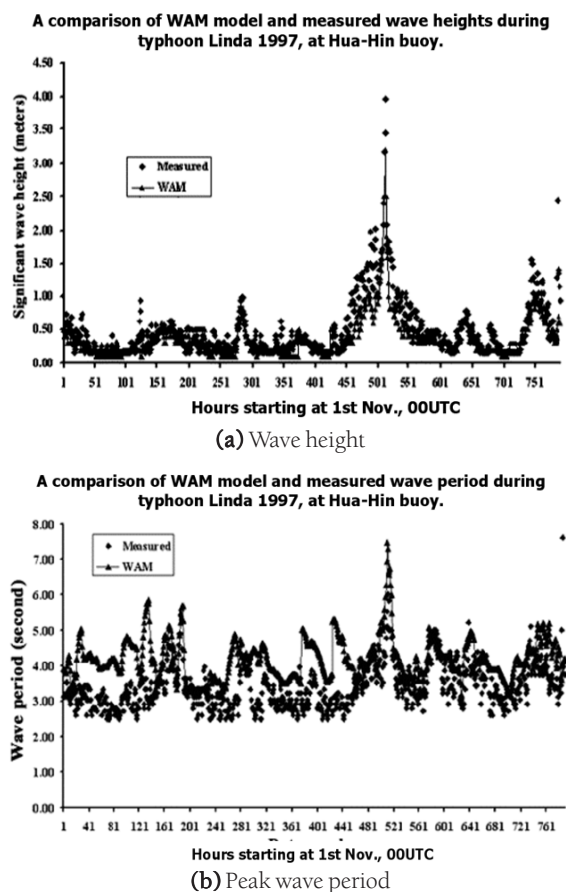
A comparison of WAM model and measured wave heights during typhoon Linda 1997, at Hua-Hin buoy.

(a) Wave height

A comparison of WAM model and measured wave period during typhoon Linda 1997, at Hua-Hin buoy.

(b) Peak wave period

Fig 6. Time series of wave parameters at HHN station.

For the GRNN, there are two models for prediction of the wave height and wave period, respectively. Each model was used to predict up to 24-hours leading time. The first model was constructed using the present values of wind velocity (U_{10}) and direction (θ_w), fetch length (F_L), significant wave height (H_s), and water depth (D_w) as inputs. The outputs are wave heights at leading time of 3, 6, 9, 12, and 24 hours. The second model was constructed in a similar way to the first model but using the wave periods instead of wave heights. The training was done for the whole period between August – December 1997. There are 1,430 data patterns used in this study covering 4 wave stations. Each model was trained by using the cross-training technique (at every 2 data patterns).

Results of simulations obtained from the GRNN are presented in Table 1. The verification statistics (by the root mean square error, RMSE, and the efficiency index, EI, as the percentage of occasions when below normal and above normal events are correctly predicted) show that the wave heights were simulated very satisfactorily when short-term prediction of less than 12 hours are concerned. In addition, the predictions with leading time of 24 hours still exhibit fairly good results. The RMSE are less than or equal to 0.15 m; the MAD are less than or equal to 0.10 m; and the EI of these forecasts are higher than or equal to 0.85, except at the KSI station where effects of wave reflection and diffraction may contribute to the errors. The wave periods were simulated not so well as wave heights. The RMSE are less than or equal to 0.4 s; the MAD are less than or equal to 0.3 s; and the EI of these forecasts are higher than or equal to 0.6.

A global evaluation of the individual forecasts is provided by the scatter plots in Fig.7, where the forecasts are compared with the observation on a one-to-one basis at the HHN station. Ideal forecasts should follow the observations exactly, and therefore all the points in the scatter plot should fall on a 1:1 line. Remarkably, for leading times up to 12 hours, the longer the predictions are performed, the more errors are observed. Figure 8 displays the time series of the wave heights and wave periods at the HHN wave stations. In general, the magnitude and phase can be simulated reasonably well. The maximum wave height obtained from the GRNN during the typhoon Linda event was found to be 4 m, which is closer to the measured data than the WAM model results.
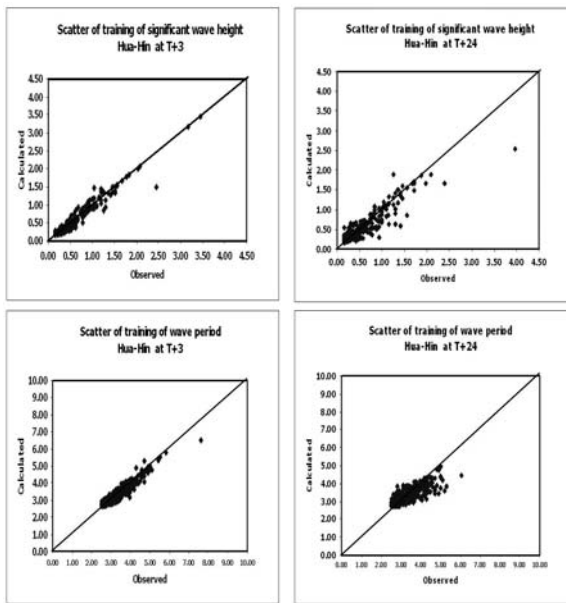
Comparisons of wave heights and wave periods are made between the WAM and GRNN at lead times of 24 hours in Table 2. It is clear that the GRNN shows better verification statistics than the WAM. Therefore, for the short-term predictions of wave parameters within 24 hours, the GRNN which is based on the concept of learning from experiences is recommended. In addition, it is also observed that the simulated results at the KSI station are not so good as at the other stations.

CONCLUSIONS

The wave fields during the attack of typhoon Linda in 1997 in the Gulf of Thailand are investigated by 2 modeling approaches. The hard computing approach by the WAM cycle 4 model was used first to simulate the wave heights and wave period distribution covering the domain 95°E to 105°E and 5°N to 15°N. Then, the soft computing approach by the GRNN model was developed to predict the wave parameters (wave heights and wave periods) for lead times of 3, 6, 9, 12, and 24

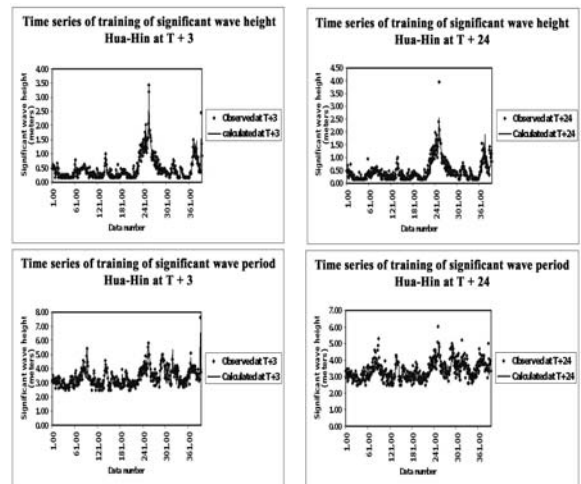**Table 1.** Results of GRNN wave parameters predictions.

Stations	Parameters	Wave height Leading time (hrs)					Wave period Leading time (hrs)				
		t+3	t+6	t+9	t+12	t+24	t+3	t+6	t+9	t+12	t+24
HHN	RMSE	0.09	0.12	0.13	0.15	0.15	0.21	0.31	0.33	0.35	0.35
	MAD	0.06	0.08	0.09	0.10	0.10	0.16	0.23	0.25	0.26	0.25
	EI	0.95	0.92	0.90	0.87	0.85	0.89	0.74	0.70	0.66	0.64
KCH	RMSE	0.06	0.09	0.11	0.12	0.14	0.19	0.26	0.30	0.30	0.33
	MAD	0.04	0.06	0.07	0.08	0.09	0.13	0.18	0.22	0.22	0.25
	EI	0.99	0.96	0.95	0.95	0.92	0.91	0.85	0.79	0.79	0.73
KSI	RMSE	0.07	0.10	0.11	0.12	0.12	0.17	0.22	0.24	0.25	0.25
	MAD	0.05	0.07	0.08	0.09	0.08	0.13	0.18	0.19	0.19	0.19
	EI	0.92	0.84	0.80	0.77	0.77	0.80	0.66	0.59	0.57	0.56
UNC	RMSE	0.06	0.09	0.10	0.11	0.14	0.17	0.24	0.26	0.30	0.34
	MAD	0.04	0.06	0.07	0.07	0.09	0.12	0.17	0.18	0.21	0.24
	EI	0.98	0.96	0.96	0.94	0.91	0.97	0.94	0.93	0.90	0.87

Fig 7. Scatter plots of wave heights and wave periods at the HHN station.

Fig 8. Time series of wave heights and wave periods at the HHN wave station.

hours. Comparisons are made among 4 wave stations.

It was found that the WAM model underestimates the wave heights. The root mean square errors (RMSE) and the mean absolute deviations (MAD) for all 4 wave stations are 0.18–0.26 m and 0.13-0.18 m, respectively. These differences between buoy data and simulated wave parameters may be due to the low spatial resolution of the employed wind fields and to the coastal boundary damping effect. The use of an analytical global wind model should improve the hindcasted waves. The wind data set that will be provided by the NRLMRY will allow more accurate simulations with nested domains. In addition, diffraction, triad-wave interactions, depth-induced breaking and bottom friction effect, are important processes in coastal regions and are not considered in WAM cycle 4.0 model. This should be an interesting alternative to reproduce wind waves in very shallow water.

The prediction accuracy of the GRNN for short lead times is quite high (RMSE < 0.15 m and MAD < 0.10 m). The magnitude and phase of wave heights and wave periods can be simulated reasonably well. However, the simulated wave periods are not so good as wave heights. The network results are also found to be more accurate than those based on the WAM model. The maximum wave height simulated by the GRNN model during the typhoon Linda event was found to be 4.0 m which is closer to the measured wave buoy data than the WAM model results. This indicates that for short-term prediction within 24 hours, the data-driven model

such as the GRNN should be viewed as a strong alternative in operational forecasting.

Table 2. Verification statistics of WAM and GRNN.

Parameters	HHN				KCH				KSI				UNC			
	Wave height		Wave period		Wave height		Wave period		Wave height		Wave period		Wave height		Wave period	
	WAM	GRNN	WAM	GRNN	WAM	GRNN	WAM	GRNN	WAM	GRNN	WAM	GRNN	WAM	GRNN	WAM	GRNN
RMSE	0.23	0.15	0.68	0.35	0.18	0.14	0.47	0.33	0.21	0.12	0.67	0.25	0.26	0.14	0.53	0.34
MAD	0.16	0.10	0.19	0.25	0.13	0.09	0.36	0.25	0.16	0.08	0.16	0.19	0.19	0.09	0.42	0.24
EI	0.68	0.85	0.58	0.64	0.87	0.92	0.46	0.73	0.28	0.77	0.58	0.56	0.69	0.91	0.67	0.87

REFERENCES

1. WAMDI group : S. Hasselmann, K. Hasselmann, E. Bauer, P.A.E.M. Janssen, G.J. Komen, L. Bertotti, P. Lionello, A. Guillaume, V.C. Cardone, J.A. Greenwood, M. Reistad, L. Zambresky and J.A. Ewing, et al (1988) The WAM Model, A third generation ocean wave prediction model, *J. Phys. Oceanogr.* **18**, 1775-810.
2. Komen, G. J., Cavaleri, L., Donelan, M., Hasselmann, K., Hasselmann, S. and Janssen, P.A.E.M. : 1994, *Dynamics and Modelling of Ocean Waves*, Cambridge University Press, 532 pp.
3. Gunther, H., S. Hasselmann and P.A.E.M. Janssen. (1991) Wamodel cycle 4. DKRZ report no. 4, Hamburg.
4. Janssen, P. A. E. M. (1991) Quasi-Linear theory of wind wave generation applied to wave forecasting; *J. Phys. Oceanogr.* **21**, 1631-42.
5. Snyder, R.L., F.W. Dobson, J.A. Elliott and R.B. Long. (1981) Array measurements of atmospheric pressure fluctuations above surface gravity waves. *J. Fluid Mech.* **102**, 1-59.
6. Janssen, P. A. E. M. (1989) Wave-induced stress and the drag of air flow over sea waves; *J. Phys. Oceanogr.* **19**, pp. 745-54.
7. Hasselmann, K. (1974) On the characterization of ocean waves due to white capping; *Boundary-Layer Meteorology*, **6**, 107-27.
8. Hasselmann, S.and Hasselmann, K. (1985) Computations and parameterizations of the nonlinear energy transfer in a gravity wave spectrum. Part I: A new method for efficient computations of the exact nonlinear transfer integral; *J. Phys. Oceanogr.* **15**(**11**), 1369-77.
9. Monbaliu, J. at al. (1998) *WAM Shallow waters version 1.00, Code changes to WAM cycle 4.0 documentation.*
10. Flood, I., and Kartam, N. (1994) Neural networks in civil engineering –I Principles and understanding, *J. Computing in Civil Engrg., ASCE*, **8(2)**, 131-48.
11. French, M.N., Krajewski, W.F., and Cuykendall, R.R. (1992) Rainfall forecasting in space and time using a neural network, *J. Hydro.***137**, 1-31.
12. Hsu, K., Gupta, H.V., and Sorooshian, S. (1995) Artificial neural networks modeling of the rainfall-runoff process, *Water Resour. Res.*, **31(10)**, 2517-30.
13. Thirumalaiah,K. and Deo, M. (1998) River stage forecasting using artificial neural networks, *J. Hydrol. Engng.*, **3(1)**, 26-32.
14. Campolo, M., Andreussi, P., and Soldati, A. (1999) River flood forecasting with a neural network model, *Water Resour. Res.*, **35**, 1191-7.
15. ASCE Task Committee on Application of Artificial Neural Networks in Hydrology. (2000a) Artificial neural networks in hydrology I : Preliminary concepts, *J. Hydrologic Engrg., ASCE*, **5(2)**, 115-23.
16. Liong, S.Y., Lim, W.H., and Paudyal, G.N. (2000) River stage forecasting in Bangladesh: Neural Network Approach, *J. Comp. in Civ. Engrg., ASCE*, **8(2)**, 201-20.
17. Hu, T.S., Lam, K.C., and NG, S.T. (2001) River flow time series prediction with a range-dependent neural network, *Hydrol. Sci. J.* **46(5)**, 729-45.
18. Vaziri, M. (1997) Prediction of Caspian sea surface water

level by ANN and ARIMA models, *J. Wtrwy., Port, Coast., and Oc. Engrg., ASCE*, **123(4)**, 158-62.

19. Deo, M.C., Naidu, C. Srihar. (1999) Real time wave forecasting using neural networks, *Journal of Ocean Engineering* **26**, 191-203.

20. Tsai, C.P. and Lee, T.L. (1999) Back-propagation neural network in tidal-level forecasting, *J. Wtrwy., Port, Coast., and Oc. Engrg., ASCE*, **125(4)**, 195-202.

21. Hsieh, B.B. and Pratt, T.C. (2001) Field data recovery in tidal system using artificial neural networks(ANNs), Coastal and Hydraulic Engineering Technical note CHETN-IV-38, U.S. Army Engineer Research and Development Center, Vicksburg, MS.

22. Lee, H.S. and Tanaka, H. (2002) Prediction of water level in a river mouth using neural network approach, Proc. 13th IAHR-APD, 669-74.

23. Specht, D.F. (1991) A general regression neural network, *IEEE trans. Neural Networks*, **2(6)**, 568-892.

24. Edwards, M.O., 1989. Global gridded elevation and bathymetry on 5-minute geographic grid, (ETOPO5). NOAA, National Geophysical Data Center, Boulder, Colorado, USA.

25. Hogan, T.F., and T.E. Rosmond, 1991: The description of the Navy Operational Global Atmospheric System's spectral forecast model.